JBC Papers in Press. Published on June 18, 2004 as Manuscript M404893200

Bistability analyses of a caspase activation model for receptor induced apoptosis*

Thomas Eißing[†‡], Holger Conzelmann[§‡], Ernst D. Gilles[§‖], Frank Allgöwer[†], Eric Bullinger[†] and Peter Scheurich[¶╫]

[†]Institute for Systems Theory in Engineering, University of Stuttgart, Pfaffenwaldring 9, 70550 Stuttgart, Germany.

[§]Institute for System Dynamics and Control, University of Stuttgart, Pfaffenwaldring 9, 70550 Stuttgart, Germany.

[‖]Max Planck Institute for Dynamics of Complex Technical Systems, Sandtorstr. 1, 39106 Magdeburg, Germany.

[¶]Institute for Cell Biology and Immunology, University of Stuttgart, Allmandring 31, 70569 Stuttgart, Germany.

[‡]These authors contributed equally to this work.

Key words: apoptosis, caspase, mathematical modeling, bistability

*This work was supported by Deutsche Forschungsgemeinschaft, Sonderforschungsbereich 495, project D2.

[╫]To whom correspondence should be addressed: Tel.: +49 711 685 6987;
Fax: +49 711 685 7484; E-mail: Peter.Scheurich@izi.uni-stuttgart.de

Running title: bistability in caspase activation

SUMMARY

Apoptosis is an important physiological process crucially involved in development and homeostasis of multicellular organisms. Although the major signaling pathways have been unraveled, a detailed mechanistic understanding of the complex underlying network remains elusive. We have here translated the current knowledge of the molecular mechanisms of the death receptor activated caspase cascade into a mathematical model. A reduction down to the apoptotic core machinery enables the application of analytical mathematical methods in order to evaluate the system behavior within a wide range of parameters. Using parameter values from literature, the model reveals an unstable status of survival indicating the need for further control. Based on recent publications we test one additional regulatory mechanism at the level of initiator caspase activation and demonstrate that the resulting system displays desired characteristics like bistability. In addition, the results from our model studies allow us to reconcile the fast kinetics of caspase 3 activation observed at the single cell level with the much slower kinetics found at the level of a cell population.

INTRODUCTION

Apoptosis is a genetically defined, major form of programmed cell death enabling the organism to remove unwanted cells, e.g. during embryonal development and after immune responses, to select educated immune cells and to eliminate virally infected and transformed cells (1,2). Enhanced or inhibited apoptotic cell death can be involved in severe pathological alterations, including developmental defects, autoimmune diseases, neurodegeneration or cancer. Extrinsic and intrinsic apoptotic pathways can be distinguished, although partly employing overlapping signal transduction pathways. A hallmark of the ongoing apoptotic process is the activation of a family of aspartate directed cysteine proteases, the caspases. Caspases are produced as proenzymes and become activated upon cleavage (3). Activation of caspases finally dismantles the cells via the cleavage of important regulatory and structural proteins and enables phagocytic removal of the dying cell (4). A simplified outline of the extrinsic pathway of apoptosis induction after death receptor stimulation is depicted in Figure 1.

Mathematical modeling and systems theory can provide valuable tools to get insight into complex dynamical systems, to test hypotheses and to identify weak points (5,6). Previous modeling approaches in apoptosis focused on the extrinsically triggered pathways, resulting in complex models (7,8). The model parameters were fitted to data derived from cell population studies showing caspase activation in the range from 30 min to several hours. These models can describe and nicely illustrate certain aspects of the signal transduction pathway. However, more recent experimental results performed at the single cell level show that the majority of caspases is activated within a very short time interval (< 15 min) (9-12).

Obviously, the single cell level is relevant for a mechanistic understanding. With the focus on receptor induced apoptosis, we used Monte Carlo methods to look for parameter domains that enable an appropriate description of apoptosis induction in a single cell (model based on Fig. 1, data not shown). The obtained results revealed an unexpected responsiveness of the system towards minute initiator caspase activation if required to act rapidly. This behavior of the model was caused by the caspase cascade itself, that

represents the main signaling route in so called type I cells (13) (Fig. 1, yellow background). We therefore translated the current picture of the extrinsically triggered caspase cascade in a very elementary form into a mathematical model enabling a thorough investigation through the application of analytical methods. Our results show that within large parameter ranges, including values from literature, this straightforward model structure is unable to appropriately describe the expected behavior that can be deduced from experimental data. We then show a way of extending our model structure to reconcile these observed differences and present a model now able to describe key characteristics like a fast execution phase and bistability. In addition, results from our model studies show a way to reconcile the fast kinetics of caspase 3 activation observed at the single cell level with the much slower kinetics found at the level of a cell population in terms of understanding and modeling.

EXPERIMENTAL PROCEDURES

The mathematical model. For each reaction considered in the Results one reaction rate can be deduced (v_1-v_{13}). The cleavage reactions (1, 2 and 4) are treated as being irreversible and it is assumed that the intermediary cleavage products ("enzyme-substrate complexes") only achieve very low levels and can thus be eliminated, reasonable estimations that have been confirmed by simulation experiments (data not shown). The reaction rate equations are deduced according to the law of mass action, which we here consider prior to other kinetic approaches, like Michaelis-Menten kinetics, although theoretical considerations show that the results would be very similar in our case. From this, molecular balances can be derived for each considered molecular species resulting in a system of ordinary differential equations (ODEs; Eq. 1-8). Two different model structures are considered in greater detail during this study. The basic model includes the reactions 1-10 and translates into the equations 1-6 (not including v_{11} in Eq. 2). The extended model hypothesis includes all reactions and translates into the complete equation system.

$$v_1 = k_1[C8^*]\cdot[C3]$$
$$v_2 = k_2[C3^*]\cdot[C8]$$
$$v_3 = k_3[C3^*]\cdot[IAP] - k_{-3}[iC3^* \sim IAP]$$
$$v_4 = k_4[C3^*]\cdot[IAP]$$
$$v_5 = k_5[C8^*]$$
$$v_6 = k_6[C3^*]$$
$$v_7 = k_7[iC3^* \sim IAP]$$
$$v_8 = k_8[IAP] - k_{-8}$$
$$v_9 = k_9[C8] - k_{-9}$$
$$v_{10} = k_{10}[C3] - k_{-10}$$
$$v_{11} = k_{11}[C8^*]\cdot[BAR] - k_{-11}[iC8^* \sim BAR]$$
$$v_{12} = k_{12}[BAR] - k_{-12}$$
$$v_{13} = k_{13}[iC8^* \sim BAR]$$

$$[\text{Eq.1}]: \frac{d[C8]}{dt} = -v_2 - v_9$$
$$[\text{Eq.2}]: \frac{d[C8^*]}{dt} = v_2 - v_5(-v_{11})$$
$$[\text{Eq.3}]: \frac{d[C3]}{dt} = -v_1 - v_{10}$$
$$[\text{Eq.4}]: \frac{d[C3^*]}{dt} = v_1 - v_3 - v_6$$
$$[\text{Eq.5}]: \frac{d[IAP]}{dt} = -v_3 - v_4 - v_8$$
$$[\text{Eq.6}]: \frac{d[C3^* \sim IAP]}{dt} = v_3 - v_7$$
$$[\text{Eq.7}]: \frac{d[BAR]}{dt} = -v_{11} - v_{12}$$
$$[\text{Eq.8}]: \frac{d[C8^* \sim BAR]}{dt} = v_{11} - v_{13}$$

The models were implemented in both Matlab (for simulation experiments) and Mathematica (for analytical analysis).

Initial conditions, parameters and units. The average concentrations in an unstimulated cell (i.e. initial conditions) of caspase 8 and 3 were quantified in HeLa cells to be 130,000 and 21,000 molecules/cell, respectively, using quantitative western blot analyses (unpublished data). The average concentration of IAPs[1] was estimated to be 40,000 molecules/cell. Other reported concentrations are 30 nM, 200 nM and 30 nM for caspase 8,

caspase 3 and XIAP respectively (14,15). Estimating a cell volume of 1 pl yields that 600 molecules per cell equals 1 nM. Accordingly, these values are roughly in the same order of magnitude and were used as initial concentrations. The other compounds were considered not to be present in the absence of a stimulus. In the extended model, the concentration of the newly introduced molecule BAR was assumed to be 40,000 molecules/cell. We consider the unit molecules/cell more illustrative for cellular concentrations than the unit M, but on the other hand we prefer and use units such as $M^{-1}s^{-1}$ for the K_m/k_{cat} ratios.

Table 1 lists the parameters as used in the "single set" simulations (unless indicated otherwise). The respective values are also provided in more common units (in brackets). For the reactions 3 and 5-10 the parameter values were taken from literature as stated in the text. The respective references are summarized in Table 2. For the reactions 1, 2 and 4 values were chosen that are in accordance with the desired kinetics and the requirement for bistability (as deduced from bifurcation analyses). The values for reaction 11 were fixed under the assumption of a similar binding affinity as reported for reaction 3. The values for the reactions 12 and 13 represent estimated turnover rates. All these data are available in a Matlab simulation file located at http://www.sysbio.de/projects/tnf/jbc.

Steady state derivation. The steady states were derived under the steady state condition dy/dt = 0 (for all compound concentrations y). A consecutive elimination of variables leads to a polynomial in C3*, whose solutions present the steady state concentrations of C3* from which the steady state concentrations of the other molecular species can be derived. The life steady state can be factored out leaving a quadratic equation of the general form $ax^2 + bx + c = 0$ for the basic model and a fourth order polynomial for the extended model. The quadratic formula was used to construct the green ($b^2 = 4ac$; saddle-node bifurcation manifold) and the blue ($-b/a = 0$) area in Figure 3. Interestingly, the coefficient c is the same as the coefficient c derived in the stability analysis (see below).

Stability analysis. For the life steady state one can construct the characteristic polynomial $\det(\lambda I - A)=0$. Here, det refers to the determinant, λ represents the Eigenvalues, I the identity matrix and A the Jacobian matrix evaluated at the life steady state. For the non-linear ODE

system to be locally (asymptotically) stable, all Eigenvalues need to have negative real parts. The Hurwitz criterion provides conditions for stability based on the coefficients of the characteristic polynomial. The most restrictive for the basic model is that the coefficient c (below) is positive, which was also used to construct the red area shown in Figure 3 (transcritical bifurcation manifold). The stability of the steady states other than the life steady state were evaluated numerically.

$$c = k_5\,(IAP\,k_3\,k_7 + k_6\,(k_7 + k_{-3})) - C3\,C8\,k_1\,k_2\,(k_7 + k_{-3})$$

Deriving an input distribution. We assume a population behavior as depicted in Figure 5A, which can be interpreted as a probability distribution. We further assume that 100 % of caspase activation corresponds to 100 % cell death, i.e. caspase 3 becomes significantly activated in every cell within the population. Further, based on the simulations of the deterministic single cell model described in Figure 4, we can describe the maximal caspase 3 activation as a function of C8* input. Hereby we assume the maximal caspase activation to define the time point of cell death. This correlates the stochastic time point of cell death to a stochastic input signal for the single cells within a population. From the original distribution of Figure 5A we thus obtain a distribution of cell death probability as a function of input activation. The corresponding probability density function can be derived by differentiation as shown in Figure 5B.

RESULTS

The biology of the model system. The type I cell-like (13) model (called basic model in the following) was constructed with the purpose of being as uncomplicated as possible without neglecting essential steps concerning our analyses (see below), i.e. simplifications represent conservative estimations. As a model input we use a pulse of activated caspase 8, which is produced by the death inducing signaling complex (DISC) formed at the membrane after death receptor stimulation (16) (although the initial steps seem to be more complex in the

case of TNFR1 (17)). The model is outlined in Figure 1 (yellow background) and contains the following reactions:

C8* + C3 → C8* + C3* [1]

C8 + C3* → C8* + C3* [2]

C3* + IAP ↔ iC3*~IAP [3]

C3* + IAP → C3* [4]

degradation & turnover reactions [5-10]

Pro-caspase 3 (C3, standing for the executioner caspases in general, e.g. caspases 3, 6 and 7) is cleaved and activated by activated caspase 8 (14,18) (C8*; standing for both initiator caspases, caspases 8 and 10) (reaction 1). Activated caspase 3 (C3*) acts in terms of a positive feedback loop onto pro-caspase 8 (C8) (19-21) (reaction 2). Here we neglect the presumably amplifying effect of caspase 6 within this feedback loop. Activated caspase 3 binds to and is inactivated by XIAP, here for simplicity termed IAP (inhibitor of apoptosis protein), as cIAP-1 and cIAP-2 also have the capacity to block caspase 3, although with less efficiency (22,23). IAP-bound, activated caspase 3 may form a pool (reaction 3), but in parallel IAP molecules can be cleaved by the activated caspase 3 (reaction 4). The cleavage products of XIAP have been described to exert only minor effects on caspase 3 (24), so these are neglected. Also, the two cleaved forms of caspase 3 are not distinguished, as both have been described to possess similar catalytic activities (15). Further on, activated caspases, as well as activated caspase 3 complexed with IAPs, are continuously degraded and pro-caspases as well as IAPs are subjected to a turnover (reactions 5-10). We thus obtain a system of 6 ODEs as detailed in the Experimental Procedures section.

Bistability and apoptosis. Several signal transduction pathways governing cell fate decisions have experimentally and theoretically been shown to display a bistable behavior (25-27). Bistability is also an obvious and mandatory property of the apoptotic machinery, as

the status “alive” must be stable and resistant towards minor, accidental trigger signals (i.e. “noise”) (28). Also, caspases are known to possess zymogenicity (18) and partial activation is observed in some physiological processes (29). However, if the apoptotic initiation signal is beyond a certain threshold, the cell must irreversibly enter the pathway to develop apoptosis. In the following, we use this information in a reverse engineering manner (6) and take bistability as a “conditio sine qua non” to evaluate possible models with respect to this expected behavior.

The basic model shows an unstable life steady state. Solving the equation system of our basic model under steady state conditions reveals three steady states. One of these, the “life steady state”, corresponds to the initial conditions in which the system remains without an external trigger, i.e. without initial caspase 8 activation. This was expected as our model parameters defining new synthesis of molecules had been chosen to balance their degradation and additional influences were neglected. The stability of the steady state provides information about the system behavior close to that steady state, indicating the response to very minor activating input signals. If the steady state is stable, the system will return to its original steady state, provided the perturbations are small enough – a situation expected for our model.

The stability of a steady state can be evaluated using the Hurwitz criterion, which is well established in systems theory (see Experimental Procedures). The point where the stability properties change, i.e. the bifurcation point, provides insight into the qualitative system behavior for certain parameter ranges. We introduced fixed parameter values for all reaction rates except for reaction 1 (Table 1), and find that the life steady state is only stable for k_1 values below ~ 3.2×10^3 $M^{-1}s^{-1}$, a value more than 300 times lower than reported in literature (14,18) (the situation is illustrated in Figure 2). Figure 3 shows the bifurcation point (red area) in dependence of three parameter classes with fixed ratios in each class. The parameter combination that can be deduced from literature (Fig. 3, yellow dot) is far away from those combinations enabling a stable life steady state (below the red area in Fig. 3). To further confirm our results, we conducted several million simulations with small inputs and

random sets of parameters taken from the parameter ranges shown in Table 2. All combinations resulted in significant caspase activation with very small input signals (i.e. an unstable life steady state), although the onset time varied greatly (data not shown).

Bistability within a small parameter domain. The two additional steady states besides the life steady state provide further information. Theoretically, one additional steady state within the positive concentration range is sufficient to achieve bistability (because other phenomena than an unstable steady state could separate the two stable steady states). However, in our model this configuration is only possible above the red area (Fig. 3, see Experimental Procedures) and for that setting the life steady state is unstable. Accordingly, bistability is only possible if both additional steady states are within the positive concentration range (above the blue area in Fig. 3). Another restriction is imposed by our biological system as the solutions must contain real numbers (above the green area in Fig. 3). Thus, bistability is only possible in a very restricted parameter area far away from values reported in literature (Fig. 3, yellow dot). In accordance with general considerations on this topic (25,30) the feedback from caspase 3 onto caspase 8 is necessary for bistability (data not shown).

IAPs and their cleavage. Interestingly, by and large the stability of the life steady state seems to be independent of the IAP cleavage reaction (Fig. 3). This is not expected and indeed dynamic simulations show that, upon faster IAP cleavage, the onset of caspase activation is achieved more rapidly for parameter combinations where the life steady state is unstable (data not shown). However, for parameter combinations where the life steady state is stable, a slower reaction stabilizes the life steady state by enlargement of its area of attraction (globally stable without this reaction). This can be explained by the fact that we assumed higher concentrations of IAPs than that of caspase 3, in order to make a conservative estimation concerning the stability of the life steady state. If we assume lower numbers of IAP molecules, we can achieve bistability (which would also require the turnover of IAPs not to exceed that of caspases significantly) even in the absence of this cleavage reaction. However, the parameters where a stable life steady state is possible, would be

even further away from those values reported in literature (data not shown). Together, the model indicates that the IAP cleavage reaction is important for a decisive switching.

Further analysis of the model reveals that apoptosis can only proceed after the IAP pool is exhausted, as otherwise most of the active caspase 3 molecules become neutralized (data not shown). As the binding of active caspase 3 to IAPs is a reversible reaction, a slower degradation of the complexes would elevate the levels of free active caspase 3 and therefore promote apoptosis. Thus, our results also argue for the view of IAPs as altruistic proteins, sacrificing themselves to prevent cell death (31). In our investigations we did not change the initial concentrations in order to restrict the number of free parameters. However, in the mathematical formulas it can be seen that changing a parameter value has similar effects as changing an initial concentration, and so we have indirectly evaluated these influences as well.

Bistability through model extension. An inherent problem of the described basic model of caspase activation is that relatively fast activation kinetics must be realized in order to be consistent with parameter values from literature and observations in various experimental setups (9-12,32,33). On the other hand, only if the kinetics are slow, the system displays the desired bistability. There are several possibilities how a model extension could reconcile those facts as described in the Discussion. One possibility is a mechanism to inhibit active caspase 8. In fact, recent reports describe that activated caspase 8 can be functionally inactivated in mitochondrial membranes. There, the molecule BAR (bifunctional apoptosis regulator) has been proposed to bind activated caspase 8 via its pseudo death effector domain leading to effective neutralization of its proteolytic activity (34-37). We therefore introduced the molecule BAR into our model, and assumed it to bind to activated caspase 8 with an affinity similar to XIAP binding to activated caspase 3 (23,38). In addition, we introduced a normal turnover rate for the new compounds (see Experimental Procedures).

The resulting system provides five steady states, two of which contain negative concentrations for the evaluated area and are thus not of interest. Importantly, stability of the life steady state of this extended model is possible with kinetic values close to those

described in literature (illustrated in Fig. 2, bifurcation point at $k_1 \approx 5.9 \cdot 10^5\ M^{-1}s^{-1}$ for other parameters as shown in Table 1). We performed simulations with input signals of different strength (Fig. 4), using a set of parameters where the system displays a bistable behavior (Table 1). In each case, caspase activity remains low for a certain time, inversely proportional to the stimulus strength, followed by a steep rise in activity if the input exceeds the threshold (about 550 molecules of activated caspase 8 per cell). After reaching a maximum, caspase activity ceases again, due to our assumption of higher degradation rates for the activated caspases as compared to the production rates of the pro-caspases. Similar to the model without the molecule BAR, the IAPs again play a critical role. Only after the IAP and the BAR pools have been exhausted, apoptosis can proceed (data not shown). Although the exact quantitative behavior depends on the choice of parameters, these simulations display the desired characteristics like bistability and fast activation kinetics combined with prolonged lag phases, inversely related to the strength of the apoptotic trigger, as observed in experiments (9).

Reconciling single cell and population studies. The model derived here has the aim to reproduce certain aspects of apoptosis induction at the single cell level. However, most experimental studies have been performed using cell populations where effector caspase activation is typically observed within a range of a few hours (13,39,40). Figure 5A shows an example of a slow time course of effector caspase activation. As described above, the strength of the apoptotic stimulus mainly translates into the delay between the apoptotic trigger and significant effector caspase activation. Thus, different delay times due to the stochastic nature of biological systems enable small fast single-cell segments of caspase activation to integrate, forming an overall slow caspase activation at the macroscopic level. Figure 5B shows the distribution of input signals into the extended BAR model (as described above) required to produce a population behavior as depicted in Figure 5A (Experimental Procedures). Although this approach is very simplified, it already reconciles single cell and population data and shows a way of combing both in terms of understanding and modeling.

DISCUSSION

In the past, systems theory has been mainly used to understand dynamic processes of technical structures, but recently it has been increasingly applied in biology (5,6). Many articles focus on the mathematical modeling of aspects of the metabolism, where (quasi) steady state approximations can be used and the mere structure provides valuable information (41). The initiation and development of apoptosis, however, is a highly dynamic process where steady state approximations cannot be easily applied. We employ a reduced model in order to evaluate the principle behavior, but also take dynamic information into account using data from various sources trying to fuse them together with the help of our model. The class of biological systems exemplified here has previously not been evaluated with respect to bistability, although bistability can be shown for special classes of larger systems (30). Our results show that (partly) analytic approaches for additional classes are feasible for larger systems than widely believed.

The present study analyses the basic core reactions of caspase activation as they are widely accepted to occur after death receptor activation (2,3,42). Because the molecular events occurring at the level of the receptor induced signaling complex are only in part understood (13,17), the input signal of the model is represented by a given number of molecules of activated initiator caspase (Fig. 1), excluding the pathways how this initial caspase activation is mediated. This model, however, reveals no stable steady state in the life status, mainly caused by the strong forward reaction of the caspase cleavage reactions as such, containing a positive feedback loop. We therefore reduced further analyses to the reactions depicted in Figure 1 on the yellow background, including the caspase activation reactions. Bifurcation analyses of this basic model reveal that it is capable to display the desired bistable behavior only within a narrow range of kinetic parameter values that are far away from values reported in literature. We thus considered possible modifications in the model structure, capable to reconcile the observed fast kinetics and tolerance to sub-threshold stimuli. A common way in cell biology to achieve such a behavior is cooperativity (25), which could also be assumed to exist for caspases, as they are known to act as

heterodimers. However, recent work shows that the monomer is just as bioactive as the dimer, arguing against this possibility (43). Alternatively, one might suggest a mechanism where not the kinetic constants are altered, but where the amount of free active caspase is limited. Such mechanisms are well known to exist for caspases 3 and 9, where IAPs lower the effective concentration of active proteases. In addition, more recent reports describe the inhibitory molecule BAR, acting at the caspase 8 level (34-37)(see Results). Based on these literature data, we extended our basic model to include BAR and the resulting model system displays the mandatory bistable behavior within a wide parameter range close to the kinetic parameter values reported in literature. Moreover, this extended model now easily describes the fast activation kinetics of caspase activation in individual cells, combined with prolonged lag phases in agreement with experimental data (9). Although additional explanations for these long lag phases have been proposed recently (at least for TNF induced apoptosis (17)), our studies demonstrate that caspase 8 capture/inactivation is a likely mechanistic explanation for the observed lag period followed by fast effector caspase activation. Whereas this lag phase might be largely controlled at the level of the mitochondria in type II cells (9,10), a similar behavior was also observed for type I cells, although initial activation of caspase 8 takes place immediately after stimulation (13,16).

In fact, in a very recent publication a new class of molecules has been described, termed caspase 8 and 10 associated RING proteins (CARPs), that are proposed to be novel caspase 8 and 10 inhibitors, acting similar to the IAP proteins (44). In the light of the results from our studies, these experimental data underscore the necessity for an effective regulation at the level of initiator caspases in death receptor mediated apoptosis. Regarding the model system, the effects of direct caspase 8 inhibition and inactivation by CARPs or their capture at the mitochondrial membranes by BAR proteins are reasonably equivalent, as the mathematical model does not take into account processes of diffusion and both mechanisms effectively lower the number of molecules of free, active initiator caspase.

In experimental studies the activation of effector caspases both in type I as well as type II cell populations occurs gradually within a few hours (13,39,40), as schematically

depicted in Figure 5A. However, at the single cell level, rapid caspase 3 activation has been observed after a lag phase in the very same experimental setup (9-12). Using our extended model, we can easily reconcile the observed fast kinetics at the single cell level with the slower rates observed in cell populations. We show here that the variation of the input signal strength within single cells, as depicted in Figure 5B, results in slow kinetics at the population level as shown in Figure 5A. The required stochastic input can be explained, for example, by different numbers of death receptors expressed in different cells, but also in a similar way by (or more likely in combination with) different numbers of BAR proteins, CARPs and other molecules involved. The number of caspase 8 inhibitors, for example, strongly influences the threshold, as also observed in siRNA experiments against CARPs (44). Together, these results demonstrate that a strongly reduced model of complex signaling networks like the apoptotic machinery already allows testing and falsifying in comparison with experimental data, leading to deeper insight into control mechanisms of complex cellular responses.

ACKNOWLEDGEMENTS

We thank the Systems Biology Group Stuttgart and Harald Wajant for fruitful discussions.

REFERENCES

1. Leist, M., and Jaattela, M. (2001) *Nat. Rev. Mol. Cell Biol.* **2**, 589-598
2. Hengartner, M. O. (2000) *Nature* **407**, 770-776
3. Thornberry, N. A., and Lazebnik, Y. (1998) *Science* **281**, 1312-1316
4. Savill, J., and Fadok, V. (2000) *Nature* **407**, 784-788
5. Kitano, H. (2002) *Nature* **420**, 206-210
6. Csete, M. E., and Doyle, J. C. (2002) *Science* **295**, 1664-1669
7. Fussenegger, M., Bailey, J. E., and Varner, J. (2000) *Nat. Biotechnol.* **18**, 768-774

8. Schöberl, B., Gilles, E. D., and Scheurich, P. (2001) *Proceedings of the International Congress of Systems Biology, Pasadena, CA*, 158-167

9. Rehm, M., Dussmann, H., Janicke, R. U., Tavare, J. M., Kogel, D., and Prehn, J. H. (2002) *J. Biol. Chem.* **277**, 24506-24514

10. Goldstein, J. C., Waterhouse, N. J., Juin, P., Evan, G. I., and Green, D. R. (2000) *Nat. Cell Biol.* **2**, 156-162

11. Luo, K. Q., Yu, V. C., Pu, Y., and Chang, D. C. (2003) *Biochem. Biophys. Res. Commun.* **304**, 217-222

12. Tyas, L., Brophy, V. A., Pope, A., Rivett, A. J., and Tavare, J. M. (2000) *EMBO Rep.* **1**, 266-270

13. Scaffidi, C., Fulda, S., Srinivasan, A., Friesen, C., Li, F., Tomaselli, K. J., Debatin, K. M., Krammer, P. H., and Peter, M. E. (1998) *EMBO J.* **17**, 1675-1687

14. Stennicke, H. R., Jurgensmeier, J. M., Shin, H., Deveraux, Q., Wolf, B. B., Yang, X., Zhou, Q., Ellerby, H. M., Ellerby, L. M., Bredesen, D., Green, D. R., Reed, J. C., Froelich, C. J., and Salvesen, G. S. (1998) *J. Biol. Chem.* **273**, 27084-27090

15. Sun, X. M., Bratton, S. B., Butterworth, M., MacFarlane, M., and Cohen, G. M. (2002) *J. Biol. Chem.* **277**, 11345-11351

16. Lavrik, I., Krueger, A., Schmitz, I., Baumann, S., Weyd, H., Krammer, P. H., and Kirchhoff, S. (2003) *Cell Death Differ.* **10**, 144-145

17. Micheau, O., and Tschopp, J. (2003) *Cell* **114**, 181-190

18. Stennicke, H. R., and Salvesen, G. S. (1999) *Cell Death Differ.* **6**, 1054-1059

19. Slee, E. A., Harte, M. T., Kluck, R. M., Wolf, B. B., Casiano, C. A., Newmeyer, D. D., Wang, H. G., Reed, J. C., Nicholson, D. W., Alnemri, E. S., Green, D. R., and Martin, S. J. (1999) *J. Cell Biol.* **144**, 281-292

20. Cowling, V., and Downward, J. (2002) *Cell Death Differ.* **9**, 1046-1056

21. Van de Craen, M., Declercq, W., Van den brande, I., Fiers, W., and Vandenabeele, P. (1999) *Cell Death Differ.* **6**, 1117-1124

22. Salvesen, G. S., and Duckett, C. S. (2002) *Nat. Rev. Mol. Cell Biol.* **3**, 401-410

23. Ekert, P. G., Silke, J., and Vaux, D. L. (1999) *Cell Death Differ.* **6**, 1081-1086

24. Deveraux, Q. L., Leo, E., Stennicke, H. R., Welsh, K., Salvesen, G. S., and Reed, J. C. (1999) *EMBO J.* **18**, 5242-5251

25. Ferrell, J. E., and Xiong, W. (2001) *Chaos* **11**, 227-236

26. Ferrell, J. E., Jr. (2002) *Curr. Opin. Cell Biol.* **14**, 140-148

27. Xiong, W., and Ferrell, J. E., Jr. (2003) *Nature* **426**, 460-465

28. Tyson, J. J., Chen, K. C., and Novak, B. (2003) *Curr. Opin. Cell. Biol.* **15**, 221-231

29. Newton, K., and Strasser, A. (2003) *Genes Dev.* **17**, 819-825

30. Angeli, D., Ferrell, J. E., Jr., and Sontag, E. D. (2004) *Proc. Natl. Acad. Sci. USA* **101**, 1822-1827

31. Ditzel, M., and Meier, P. (2002) *Trends Cell Biol.* **12**, 449-452

32. Krippner-Heidenreich, A., Tubing, F., Bryde, S., Willi, S., Zimmermann, G., and Scheurich, P. (2002) *J. Biol. Chem.* **277**, 44155-44163

33. Fladmark, K. E., Brustugun, O. T., Hovland, R., Boe, R., Gjertsen, B. T., Zhivotovsky, B., and Doskeland, S. O. (1999) *Cell Death Differ.* **6**, 1099-1108

34. Qin, Z. H., Wang, Y., Kikly, K. K., Sapp, E., Kegel, K. B., Aronin, N., and DiFiglia, M. (2001) *J. Biol. Chem.* **276**, 8079-8086

35. Zhang, H., Xu, Q., Krajewski, S., Krajewska, M., Xie, Z., Fuess, S., Kitada, S., Pawlowski, K., Godzik, A., and Reed, J. C. (2000) *Proc. Natl. Acad. Sci. USA* **97**, 2597-2602

36. Breckenridge, D. G., Nguyen, M., Kuppig, S., Reth, M., and Shore, G. C. (2002) *Proc. Natl. Acad. Sci. USA* **99**, 4331-4336

37. Stegh, A. H., Barnhart, B. C., Volkland, J., Algeciras-Schimnich, A., Ke, N., Reed, J. C., and Peter, M. E. (2002) *J. Biol. Chem.* **277**, 4351-4360

38. Deveraux, Q. L., Takahashi, R., Salvesen, G. S., and Reed, J. C. (1997) *Nature* **388**, 300-304

39. Fotin-Mleczek, M., Henkler, F., Samel, D., Reichwein, M., Hausser, A., Parmryd, I., Scheurich, P., Schmid, J. A., and Wajant, H. (2002) *J. Cell Sci.* **115**, 2757-2770

40. Hentze, H., Schmitz, I., Latta, M., Krueger, A., Krammer, P. H., and Wendel, A. (2002) *J. Biol. Chem.* **277**, 5588-5595

41. Stelling, J., Klamt, S., Bettenbrock, K., Schuster, S., and Gilles, E. D. (2002) *Nature* **420**, 190-193

42. Ashkenazi, A. (2002) *Nat. Rev. Cancer* **2**, 420-430

43. Donepudi, M., Mac Sweeney, A., Briand, C., and Grutter, M. G. (2003) *Mol. Cell* **11**, 543-549

44. McDonald, E. R., 3rd, and El-Deiry, W. S. (2004) *Proc. Natl. Acad. Sci. USA* **101**, 6170-6175

45. Garcia-Calvo, M., Peterson, E. P., Rasper, D. M., Vaillancourt, J. P., Zamboni, R., Nicholson, D. W., and Thornberry, N. A. (1999) *Cell Death Differ.* **6**, 362-369

46. Yoo, S. J., Huh, J. R., Muro, I., Yu, H., Wang, L., Wang, S. L., Feldman, R. M., Clem, R. J., Muller, H. A., and Hay, B. A. (2002) *Nat. Cell Biol.* **4**, 416-424

FOOTNOTES

[1]The abbreviations used are: BAR, bifunctional apoptosis regulator; CARP, caspase 8 and 10 associated RING proteins; Cn, pro-caspase n; Cn*, activated caspase n; IAP, inhibitor of apoptosis protein; ODE, ordinary differential equation. Supplementary information is available at: http://www.sysbio.de/projects/tnf/jbc.

FIGURE LEGENDS

FIG 1. **Outline of apoptotic pathways downstream of death receptors.** Initially, partial activation of caspase 8 (C8*, the active status of caspases is indicated by an asterisk) is mediated by death receptor stimulation. C8* can cleave and activate caspase 3 (C3) directly but also cleaves Bid to release t-Bid. Mitochondrial t-Bid (t-BidM) leads to the release of cytochrome c (cytC) and Smac/DIABLO (Smac). Caspase 9 (C9) is activated by cytC and activates C3. C3* can activate residual C8 in a feedback loop. C9* and C3* can be inhibited by inhibitor of apoptosis protein (IAP) molecules and subsequently fed into proteasomal degradation. Mitochondrially released Smac competes with the caspases for IAP binding and degradation.

FIG 2: **Bifurcation illustration.** A steady state implies that the concentrations of the compounds within the system do not change over time. If we start at close-by concentrations, the system will move back into the steady state if it is stable, but move away if it is unstable. Here the steady states and their stability properties in dependence of the reaction rate k_1 are illustrated schematically, with the other parameters kept constant. The third coordinate can be envisioned as energy and was introduced to add plasticity. Solid lines indicate stable, dashed lines unstable steady states. For small values of k_1 we find a landscape of a bistable system with a stable life steady state (black line), a stable apoptotic steady state (green line) and a third unstable steady state separating the two areas of attraction (red line). When the parameter k_1 increases, the landscape changes as the unstable separating steady state meets with the stable life steady state. At this bifurcation point the two steady states exchange their stability properties and the formerly separating steady state vanishes into the biologically not relevant negative concentration area. Thus, for larger values of k_1 we find an unstable life steady state with the stable apoptotic steady state being attractive in the whole positive concentration area.

FIG 3: **(Bi-)Stability analysis.** Stability aspects of the basic model were evaluated over wide parameter ranges. For the three-dimensional visualization the following parameter ratios were chosen as axis: for caspase activation $k_1 = 2 \cdot k_2$, for half-life time $k_7 = k_8 = 2 \cdot k_5 = 2 \cdot k_6 = 4 \cdot k_9 = 4 \cdot k_{10}$, and for IAP cleavage k_4; v_3 was fixed according to literature values. The yellow dot indicates values as expected from literature data (although the IAP cleavage reaction parameter can only be estimated, see Table 2). Above the red area no stable life steady state exists, below the blue area no second stable steady state within the positive concentration range can exist and below the green area the solutions are complex numbers. Thus, bistability requires parameter combinations below the red AND above the blue AND above the green area.

FIG 4: **Bistable behavior of the extended model.** Simulation experiments with varying inputs (initial C8* concentrations) and C3* over time as output are shown. Above a certain input threshold (~ 550 molecules of C8*) the system becomes fully activated, while sub-threshold activation results in recovery. The two stable steady states can be envisioned, with the life steady state corresponding to the blue area and the apoptotic steady state corresponding to the green area achieved after longer time periods.

FIG 5: **Reconciling single cell and populations kinetics. A** shows an idealized time course of caspase 3 activation as observed at the population level. **B** shows the density function of the input signal necessary to achieve the population behavior depicted in A, based on single cells behaving as described in Figure 4.

Table 1

Simulation parameters. Parameter values as used in the single set simulation experiments are given (mo = molecules). In brackets the values are shown in more common units to enable direct comparison with literature values presented in Table 2. For further information see the Experimental Procedures.

	value	**unit**		**value**	**unit**
k_1	$5.8 \cdot 10^{-5}$ *(5.8·10^5)*	cell·min^{-1}·mo^{-1} *($M^{-1}s^{-1}$)*	k_{-1}	0	
k_2	10^{-5} *(10^5)*	cell·min^{-1}·mo^{-1} *($M^{-1}s^{-1}$)*	k_{-2}	0	
k_3	$5 \cdot 10^{-4}$ *($5 \cdot 10^6$)*	cell·min^{-1}·mo^{-1} *($M^{-1}s^{-1}$)*	k_{-3}	0.21 *(0.035)*	min^{-1} *(s^{-1})*
k_4	$3 \cdot 10^{-4}$ *($3 \cdot 10^6$)*	cell·min^{-1}·mo^{-1} ($M^{-1}s^{-1}$)	k_{-4}	0	
k_5	$5.8 \cdot 10^{-3}$ *(120)*	min^{-1} *(min)*	k_{-5}	0	
k_6	$5.8 \cdot 10^{-3}$ *(120)*	min^{-1} *(min)*	k_{-6}	0	
k_7	$1.73 \cdot 10^{-2}$ *(40)*	min^{-1} *(min)*	k_{-7}	0	
k_8	$1.16 \cdot 10^{-2}$ *(60)*	min^{-1} *(min)*	k_{-8}	464 *($1.3 \cdot 10^{-11}$)*	mo·cell^{-1}·min^{-1} *($M \cdot s^{-1}$)*
k_9	$3.9 \cdot 10^{-3}$ *(180)*	min^{-1} *(min)*	k_{-9}	507 *($1.4 \cdot 10^{-11}$)*	mo·cell^{-1}·min^{-1} *($M \cdot s^{-1}$)*
k_{10}	$3.9 \cdot 10^{-3}$ *(180)*	min^{-1} *(min)*	k_{-10}	81.9 *($2.3 \cdot 10^{-12}$)*	mo·cell^{-1}·min^{-1} *($M \cdot s^{-1}$)*
k_{11}	$5 \cdot 10^{-4}$ *($5 \cdot 10^6$)*	cell·min^{-1}·mo^{-1} *($M^{-1}s^{-1}$)*	k_{-11}	0.21 *(0.035)*	min^{-1} *(s^{-1})*
k_{12}	10^{-3} *(693)*	min^{-1} *(min)*	k_{-12}	40 *($1.1 \cdot 10^{-12}$)*	mo·cell^{-1}·min^{-1} *($M \cdot s^{-1}$)*
k_{13}	$1.16 \cdot 10^{-2}$ *(60)*	min^{-1} *(min)*	k_{-13}	0	

Table 2

Unstability ranges. Parameter ranges that do not provide parameter combinations enabling a stable life steady state. The k_--column indicates whether a reaction (see Experimental Procedures) is assumed to be reversible or not. If reversible, the values can be calculated with the help of the provided explanations. The last column also provides literature parameter values and the respective references.

	k_+min [$M^{-1}s^{-1}$]	**k_+max [$M^{-1}s^{-1}$]**	**k_- [s^{-1}]**	**Explanations and References**
v_1	$3 \cdot 10^4$	$5 \cdot 10^6$	no	*in vitro* $K_M/k_{cat} = 10^6$ $M^{-1}s^{-1}$ (14,18)
v_2	$2 \cdot 10^4$	$5 \cdot 10^6$	no	C3* faster than C8* using fluorogenic substrates (18,21,45)
v_3	$1 \cdot 10^5$	$5 \cdot 10^6$	yes[§]	[§]to obtain: *in vitro* $K_i = 0.7$ nM (23,38)
v_4	$1 \cdot 10^3$	$5 \cdot 10^6$	no	estimation
	$t_{1/2}$min [min]	$t_{1/2}$max [min]	k_- [$M \cdot s^{-1}$]	k_+ [min^{-1}] = $ln2/t_{1/2}$
v_5	30	300	no	$t_{1/2}$ ~ 180 min for caspases; $t_{1/2}$ = 30 - 40 min for DIAP (31,46) production rate to establish the initial concentration
v_6	30	300	no	
v_7	30	300	no	
v_8	30	300	yes	
v_9	60	500	yes	
v_{10}	60	500	yes	

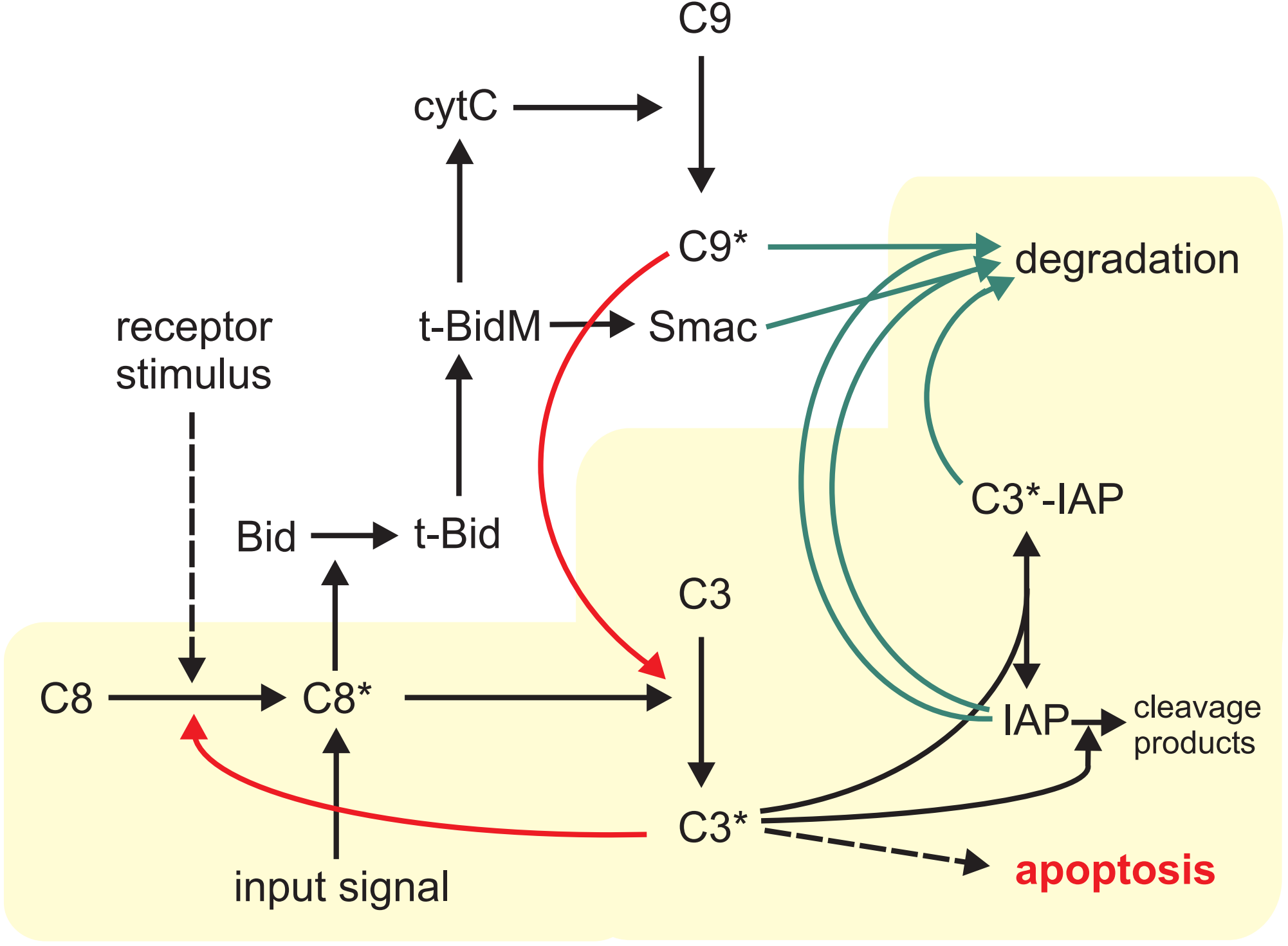
C9
cytC
C9*
degradation
receptor
stimulus
t-BidM
Smac
C3*-IAP
Bid
t-Bid
C3
C8
C8*
IAP
cleavage
products
C3*
input signal
apoptosis

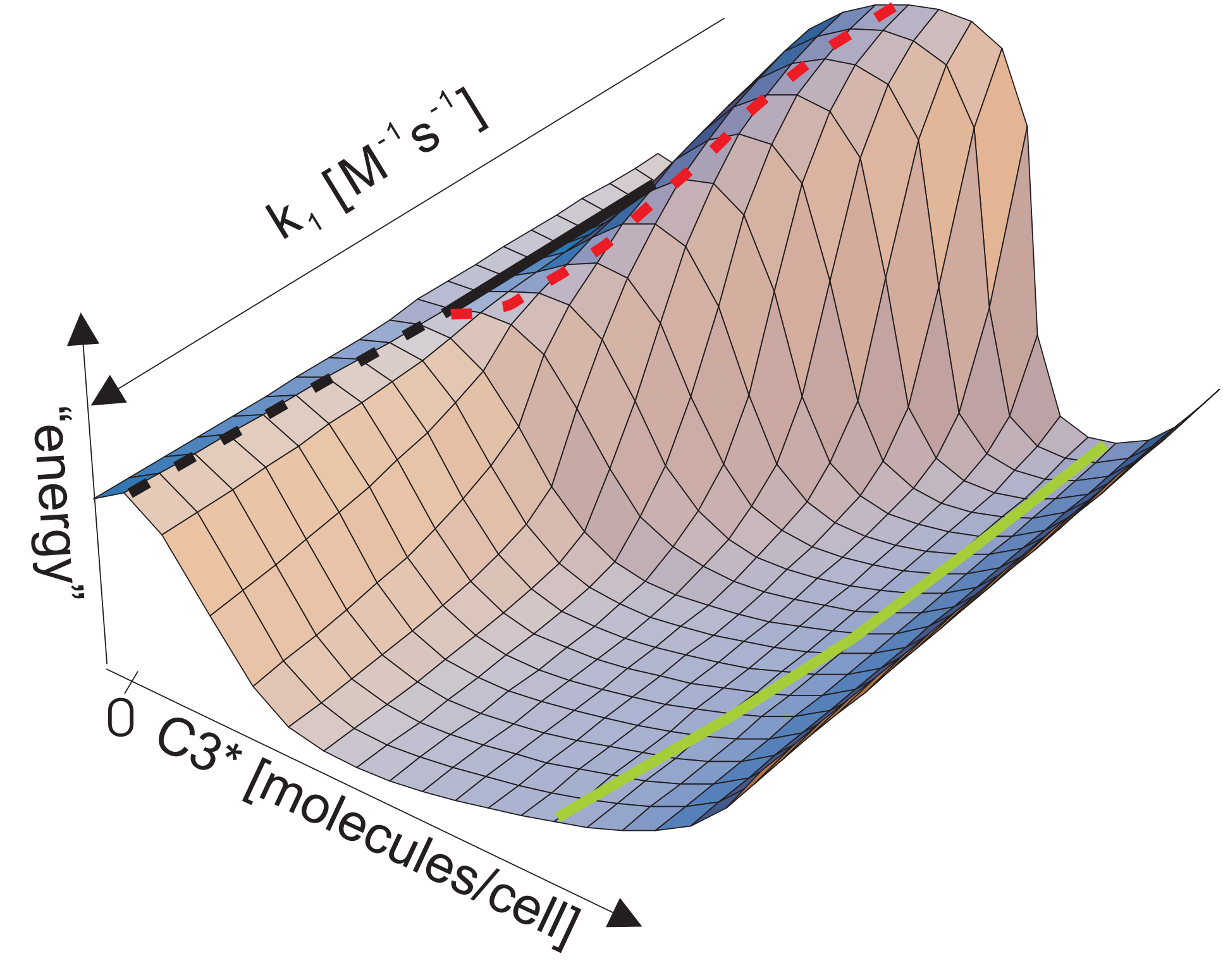
k_1 [$M^{-1} s^{-1}$]
"energy"
0
C3* [molecules/cell]

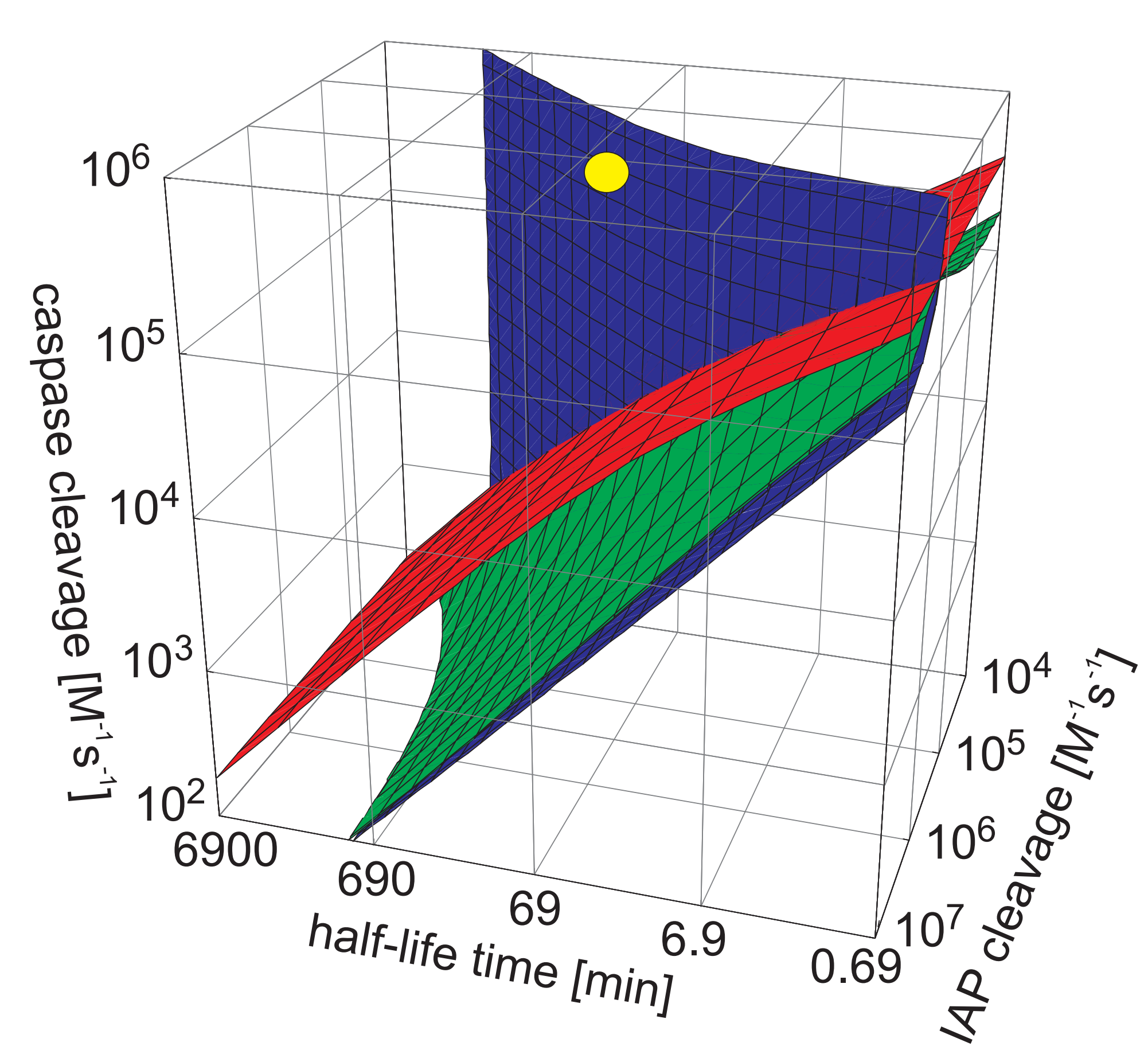
caspase cleavage [M-1s-1]
10^6
10^5
10^4
10^3
10^2
6900
690
69
6.9
0.69
half-life time [min]
10^4
10^5
10^6
10^7
IAP cleavage [M-1s-1]

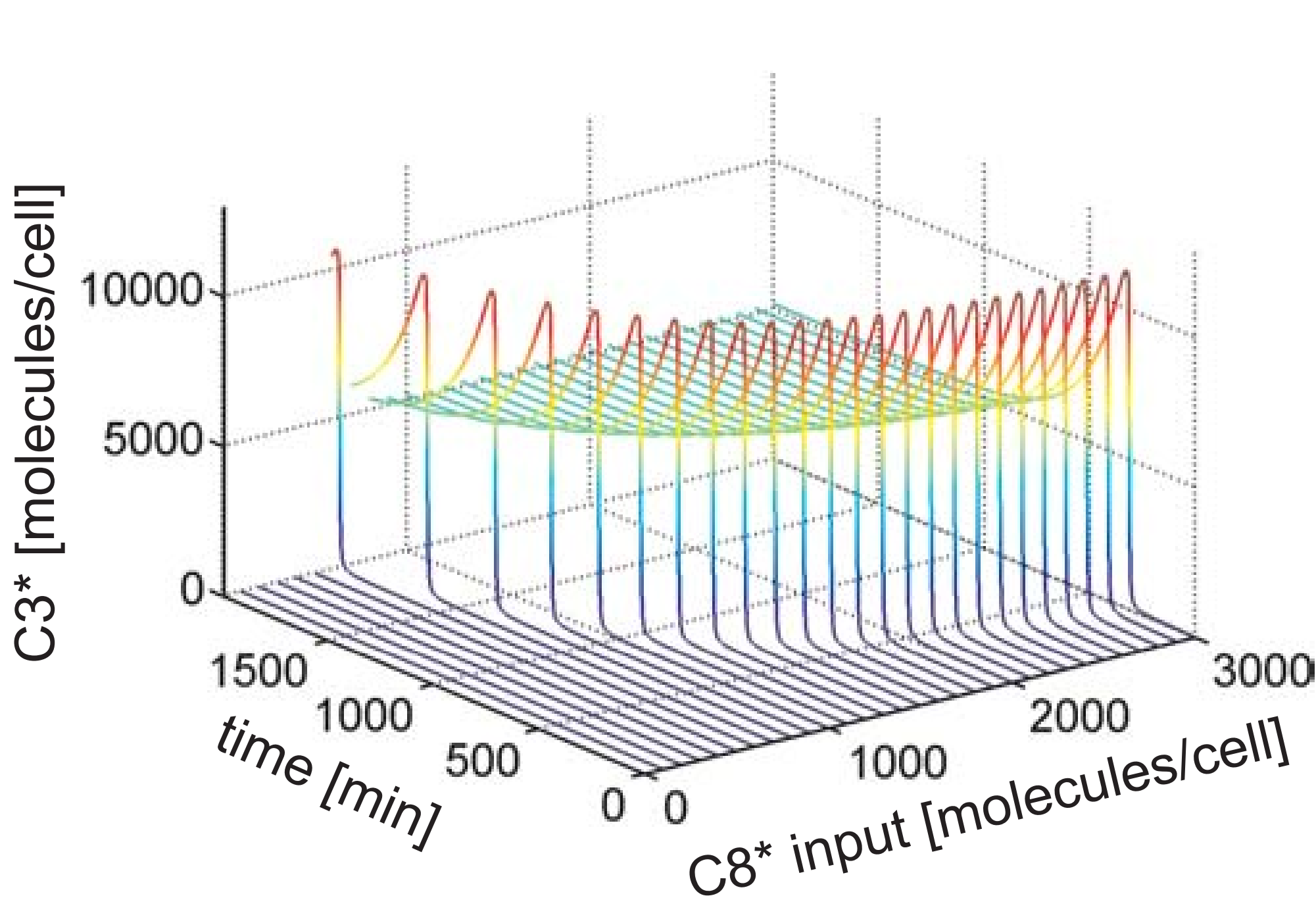
C3* [molecules/cell]
10000
5000
0
1500
1000
500
0
time [min]
0
1000
2000
3000
C8* input [molecules/cell]

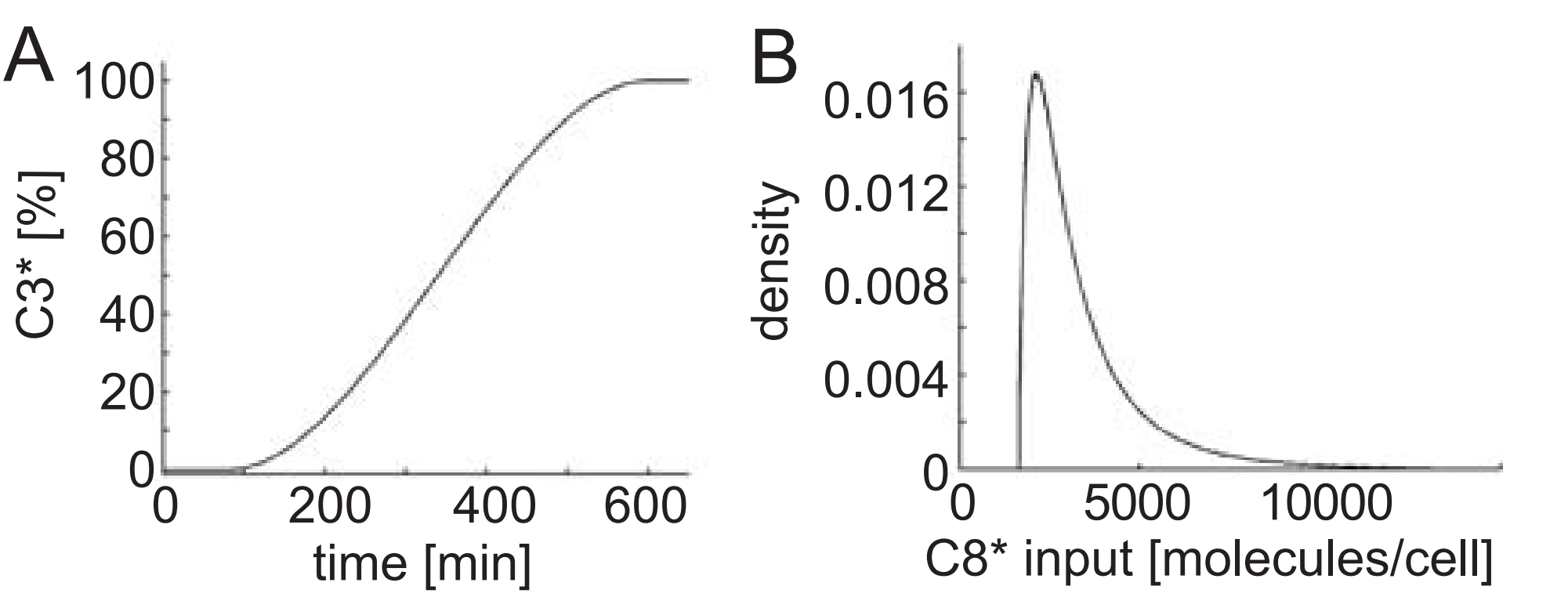
A
100
80
60
40
20
0
C3* [%]
0
200
400
600
time [min]
B
0.016
0.012
0.008
0.004
0
density
0
5000
10000
C8* input [molecules/cell]